Polymer Chemistry

Accepted Manuscript

ROYAL SOCIETY OF CHEMISTRY

www.rsc.org/polymers

For Table of Contents use Only

Marco Albuszis, Peter. J. Roth, Werner Pauer, and Hans-Ulrich Moritz

Macroporous Uniform Azide- and Alkyne-functional Polymer Microspheres with Tuneable Surface Area: Synthesis, In-depth Characterization and *Click*-Modification

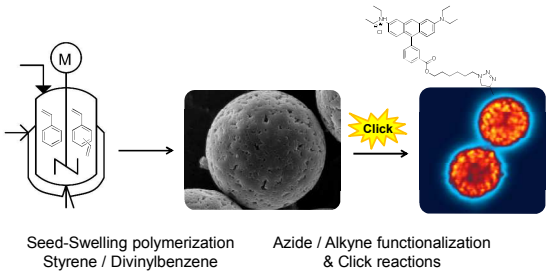

With surface areas of up to 467 m²/g, crosslinked azide- and alkyne-functional poly(styrene-*co*-divinylbenzene) microparticles enable versatile modification throughout the particle

Macroporous Uniform Azide- and Alkyne-functional Polymer Microspheres with Tuneable Surface Area: Synthesis, In-depth Characterization and *Click*-Modification

Marco Albuszis,[†] Peter. J. Roth,[‡,*] Werner Pauer,[†,*] and Hans-Ulrich Moritz[†,*]

[†] Institute for Technical and Macromolecular Chemistry, University of Hamburg, Bundesstraße 45, 20146 Hamburg, Germany

[‡] Centre for Advanced Macromolecular Design (CAMD), School of Chemical Engineering, University of New South Wales, UNSW Sydney, NSW 2052, Australia

Corresponding Author Email Addresses: P. J. Roth (p.roth@unsw.edu.au), W. Pauer (pauer@chemie.uni-hamburg.de), H.-U. Moritz (moritzhu@chemie.uni-hamburg.de)

Keywords macroporous microparticles, azide–alkyne click chemistry, high surface area, poly(styrene- divinylbenzene)

Abstract A series of uniform, macroporous poly(styrene-*co*-divinylbenzene) microspheres with diameters ranging from 6.6 ±0.2 to 8.6 ±0.2 μm was prepared in a multistep procedure involving precipitation polymerization synthesis of polystyrene seed particles, swelling of seed particles with plasticiser and porogen, and polymerization of styrene–divinylbenzene (S–DVB) inside the seed particles. Particles prepared with varying DVB feed ratios had comparable diameters (as evidenced by scanning electron microscopy) with specific surface areas increasing with DVB content from 11 to 467 m^2/g (measured by nitrogen adsorption). Residual double bonds were converted into azide functionality (through HBr addition and bromo–azide substitution) or alkyne functionality (Br_2 addition followed by double elimination) which allowed for CuAAC-click chemistry conjugation with reagents carrying the respective complimentary alkyne or azide functional groups including the fluorescent dye derivatives 7-nitro-4-(prop-2-ynylamino)benzofuran (NBD-alkyne) and Rhodamine B hexylazide synthesised for this purpose. Efficiency of chemical transformations was determined using a combination of CHN and IC elemental analyses, solid state NMR spectroscopy, FT-IR spectroscopy, Raman spectroscopy, and confocal scanning fluorescence microscopy. Although the respective seconds steps in each modification route (substitution and elimination) suffered from lower yields (~35%), porous particles with azide loadings of up to 0.71 mmol/g and alkyne loadings of up to 0.78 mmol/g were prepared. Confocal laser scanning microscopy on Rhodamine B-labelled microspheres indicated functionalization throughout the particles featuring a core–shell structure with higher functionalization in the outer layer of particles. Results are expected to contribute to the development of advanced, well-defined, macroporous particles with high, chemically accessible surface areas.

Introduction

Over the last decades macroporous, crosslinked polymer particles with narrow size distribution have been intensively studied. Owing to desirable characteristics such as high specific surface area, tuneable pore morphology, mechanical stability, and strong adsorption capacity,[1-3] such particles have found wide-spread application, for example as ion exchange resins, chromatographic packing materials for size exclusion and affinity liquid chromatography[4-8] and for immobilization of enzymes and catalysts.[9-11] Well-defined, crosslinked macroporous polymer particles in a micrometre size range are, however, not efficiently obtained through conventional one-step emulsion, dispersion, or suspension polymerization techniques.[12] While emulsion polymerization does not lend itself well to the production of porous particles from many common monomers such as styrene, dispersion and suspension methods typically provide poor control over crosslinking density and size distribution.[13] These problems were overcome with Ugelstad's "activated swelling" method. This multi-step process uses monodisperse seed particles typically submicron-sized, composed of polystyrene, and obtained through an emulsion polymerization in a subsequent suspension process in which the seed particles are swollen with monomer producing uniform compact or porous particles.[14-17] Another approach presented by Okubo et al. termed "dynamic swelling method" is based on Ugelstad's swelling principle but does not require an activating agent such as dibutylphthalate (which in Ugelstad's protocol enhances swelling) and works in a one-step process leading to highly monodisperse latex particles.[18-20] These seed–swelling polymerizations have proven to be a very versatile and efficient process in the preparation of narrow size distribution microspheres offering a large amount of control over degree of

crosslinking, porosity, and particle size.[8, 21-23] Recently, microfluidic setups have been investigated for the preparation of well-defined solid or porous polymer particles, typically in the size range of several hundreds of micrometres.[12, 24, 25]

For a range of applications, especially such involving immobilization of enzymes or catalysts, chemical functionalization of surfaces is crucial. For polystyrene-based polymer latexes (the most frequently studied material in this field) a wide variety of strategies for surface functionalization has been described. One option involves the terpolymerization of styrene and crosslinker (typically divinylbenzene) with a functional monomer such as chloromethylstyrene[26, 27] or aminomethylstyrene[28] followed by postpolymerization modification of the chloromethyl or amino groups, respectively. However, terpolymerization kinetics and compatibility of functional monomer with the polymerization process must be taken into consideration in these cases. Conventionally, functionality has also been installed into pre-made poly(styrene-*co*-divinylbenzene) particles,[29] for example by means of chloromethylation[30, 31] or aminomethylation of the styrene segments.[32] This strategy gives access to the same range of substitution and coupling reactions as the above-mentioned techniques while avoiding a terpolymerization protocol.[33] Finally, poly(styrene-*co*-divinylbenzene) particles typically contain a considerable amount of unreacted vinyl groups which provide a convenient handle for a range postpolymerization modification reactions, including radical and thermal additional reactions[34] such as bromohydration,[35] bromination,[35] epoxidation,[36] and thiol–ene reactions.[37]

A very versatile coupling reaction is the Huisgen 1,3-dipolar cycloaddtion of azides and alkynes. Following first reports on rate acceleration through catalysis in the early 2000s,

copper catalysed azide–alkyne cycloaddition (CuAAC) has become the focus of intense research.[38] Undoubtedly owing to its high robustness, tolerance to functional groups and solvents, starting material accessibility and reaction efficiency, this type of click chemistry has found its way into the polymer chemistry arena opening novel routes for the tailored design of functional macromolecules.[39-43] Several studies have detailed the success of this chemistry in the surface functionalization of (non-porous) microparticles.[44] For example, Karagöz et al.[45] subjected the remaining double bonds in poly(divinylbenzene) particles to hydrobromination followed by bromide substitution by sodium azide generating azide-functional microspheres which were coupled by CuAAC with alkyne-modified pyrene yielding fluorescently labelled particles. In a further example of click surface modification Goldmann et al.[37] employed radical thiol–ene reactions to graft thiols to the residual double bonds in poly(ethylstyrene-*co*-divinylbenzene) microspheres. Utilising 1-azido-undecane-11-thiol, azide functionality was instilled into the particle surface allowing for a coupling of an alkyne terminated polymer via CuAAC click chemistry.

However, only few reports have addressed click-modification of *porous* polymer particles; examples include porous amino agarose beads chemically modified to carry azides or alkynes,[6] argopore resins whose amino groups were converted into azides[46] and microfluidically prepared crosslinked poly(glycidyl methacrylate) after ring-opening of the epoxide groups with azide.[47] Presence and size of pores in microparticles has, however, been shown to have an enormous impact on their performance in applications, for example in enzyme immobilization, due to differences in accessible surface area.[1] We also note that the majority of studies on click-modification of particle surfaces approaches this by introducing azide functionality into the

particle, while generation of alkyne functionality, especially on polystyrene-based particles, is underrepresented in the literature. Herein, we describe a multi-step preparation of macroporous poly(styrene-divinylbenzene) microspheres with diameters of 6.6–8.6 μm and specific surface areas ranging between 11 and 467 m^2/g and the transformation of residual double bonds into azide or alkyne functionality, followed by CuAAC modification. A range of analytical tools were used to monitor each chemical modification and to estimate molar percentage and mass loadings of functionality. Two-step transformation into alkynes was found to proceed with higher overall yield than the likewise two-step transformation into azide functionality. Confocal scanning microscopy measured on alkyne-functional particles clicked with a Rhodamine B azide reagent suggested functionalization throughout the particles with a higher degree of functionalization within the outer, ~1 μm thick, layer of particles. With limited documentation on click-functionalization of porous microparticles, especially on the production of surface-bound alkyne functionality this study provides first detailed evidence of efficiency of transformations and will aid in the development of advanced functional particles for many of the above mentioned applications.

Experimental Section

Materials. Unless otherwise noted, chemicals were purchased from Sigma Aldrich, Merck Chemicals, or Acros Organics in analytical grade and were used without further purification. Styrene (S) was distilled in vacuum to remove inhibitors and impurities directly before use. 2,2'-Azobis-(2-isobutyronitril) (AIBN) was recrystallized from methanol. Divinylbenzene (DVB) was of technical grade containing 55 wt% divinylbenzene monomers and predominantly 3/4-ethyl-vinylbenzene impurity.

Polystyrene Seed Particles. In a typical experiment, polystyrene (PS) seed microspheres with a diameter of 2.8 µm and narrow size distribution were obtained by using a 3-necked 250 mL double-walled reaction flask connected to a recirculating heater and placed on a shaking plate without additional mechanical stirring. At room temperature ethanol (120 mL), polyvinylpyrrolidone (PVP-K30, M_n = 40 kg/mol, 3 g) and Aliquat 336 (1.2 g) were mixed in the reactor with shaking at 150 rpm and the mixture was purged for 15 minutes with argon before the temperature was increased to 70 °C. In a separate flask styrene (30 g) and AIBN (0.6 g) were mixed and purged with argon for 10 minutes before adding the resulting solution into the preheated reactor. The reactor was sealed and polymerization was continued for 24 h at a shaking rate of 150 rpm and stopped by cooling to room temperature. Seed latex particles were purified by repeated centrifugation using ethanol (1×), hot water (1×), and ethanol (1×) for redispersing, followed by drying in vacuum.

Uniform Crosslinked Porous Microspheres (1). Poly(styrene-*co*-divinylbenzene), P(S-DVB), microspheres were obtained in analogy to a literature procedure.[48] Seed particles with a diameter of 2.8 µm (1 g) were dispersed in 0.25 % aqueous sodium dodecylsulfate (SDS) solution (9 g) using sonication and were added to a sonicated emulsion of dibutylphthalate (DBP,

2.5 g) in 0.25 % SDS solution (50 mL). The combined mixture was stirred at 300 rpm until all small emulsion droplets of DBP had disappeared and the particles had swollen to a diameter of 4.2 μm (monitored by optical microscopy, see supporting information). Then a separately prepared emulsion containing S and DVB (in varying amounts as discussed in the text; 6 g total), toluene (4 g), benzoylperoxide (BPO, 0.25 g), and 0.25 % aqueous SDS solution (60 mL) was added to the DBP-swollen particles. The swollen particle–monomer mixture was stirred for 24 h at room temperature before the particles were stabilized by the addition of 10 wt% aqueous polyvinylalcohol (Mowiol 18-88, 10 g). The mixture was purged with argon for 15 min and transferred into a degassed, doubled-walled reactor as described above preheated to 70 °C and shaken at a rate of 150 rpm. Polymerization was allowed to proceed for 24 h. Microspheres were isolated by centrifugation and soxhlet extraction with water (24 h) and THF (24 h) to remove seed polymer, stabilizer and other additives and impurities. Finally, particles were dried in vacuum at 80 °C and were obtained as a low density white powder. Quantitative analysis by solid state NMR of particles obtained from 100% DVB indicated 56% of original double bonds remaining, corresponding to a crosslinking degree of 24% (taking the 55% grade of DVB into account), and a concentration of active sites of 2.37 mmol/g double bonds. Particles obtained from S–DVB 50:50 had 69% of original double bonds remaining, corresponding to a crosslinking degree of 7.5% and a concentration of 1.47 mmol/g double bonds. ^{13}C-SSNMR (101 MHz) δ/ppm = 144, 127 (Ar), 137 (residual vinyl Ar–*C*H=CH_2), 112 (residual vinyl Ar–CH=*C*H_2), 40 (backbone), 28 (3/4-ethyl-vinylbenzene Ar–*C*H_2–CH_3), 15 (3/4-ethyl-vinylbenzene Ar–CH_2–*C*H_3). %). FT-IR, ν/cm^{-1} = 902 (C=C); Elemental Analysis: 100% DVB; C: 88.3 %, H: 8.1%. 50% DVB; C: 91.1 %, H 8.0 %.

1-Bromoethyl-functional Particles through Hydrobromination of Residual Double Bonds (2).[45] Porous crosslinked P(S-DVB) particles (3 g) were suspended in *n*-hexane (150 mL) in a sealed flask with gas inlet and gas outlet. In a separate sealed flask equipped with a dropping funnel and connected with a tube to the gas inlet of the reaction flask concentrated sulfuric acid (10 mL, 0.18 mol) was dropped slowly onto solid KBr (29.7 g, 0.25 mol). Bubbling with HBr gas was continued for 8 h. Particles were then washed exhaustively with *n*-hexane, aqueous NaOH, H_2O, ethanol, and acetone (150 mL each), and dried in vacuum to obtain a slightly brown powder. ^{13}C-SSNMR (101 MHz) δ/ppm = 26 (–CHBr–*C*H_3); Elemental Analyses: 100% DVB; C: 71.5 %, H: 6.4 %, Br: 20.1 %. 50% DVB; C: 80.7 %, H 6.9 %, Br: 11.0%.

1-Azidoethyl-functional Particles (3). Hydrobrominated particles (3 g) were suspended in a mixture of sodium azide (0.75 g), water (5 mL), and DMF (50 mL) and stirred for 24 h at room temperature. The product was isolated by washing with DMF (100 mL), water (200 mL), ethanol (200 mL), and acetone (200 mL) and was dried in vacuum to give a white powder. ^{13}C-SSNMR (101 MHz) δ/ppm = 61 (*C*N_3); FT-IR, ν/cm^{-1} = 2101 (C–N_3 stretch); Elemental Analyses: 100% DVB; C: 75.0 %, H: 6.7%, N: 3.0 %, Br: 13.0 %. 50% DVB; C: 82.5 %, H 7.1 %, N: 1.8 %, Br: 8.0%.

1,2-Dibromoethyl-functional Particles through Bromination of Residual Double Bonds (4). Porous crosslinked P(S-DVB) particles (3 g) were suspended in chloroform (50 mL) at 0 °C and bromine (3 mL, 0.12 mol) dissolved in chloroform (20 mL) was slowly added. The mixture was stirred for 1.5 h at 0 °C, allowed to warm to room temperature, and stirred for another 24 h before pouring on ice water (100 mL). The crude product was filtered, exhaustively washed with chloroform and water, redispersed in chloroform (50 mL) and stirred for 30 minutes. After centrifugation and washing with water the slightly brown product was dried in vacuum.

Elemental Analyses: 100% DVB; C: 65.6 %, H: 5.8%, Br: 27.0 %. 50% DVB; C: 71.6 %, H 6.0 %, Br: 21.0 %.

Alkyne-functional Particles through Double Dehydrohalogenation (5). Brominated particles (3 g) were suspended in a mixture of potassium hydroxide (17 g) and absolute ethanol (50 mL). The mixture was refluxed at 95 °C with stirring overnight. After cooling to room temperature water (50 mL) was added followed by filtration and washing the particles with water, aqueous HCl, water, ethanol, and acetone (200 mL each) before drying in vacuum. ^{13}C-SSNMR (101 MHz) δ/ppm = 84 (Ar–*C*≡CH), 76 (Ar–C≡*C*H). Elemental Analyses: 100% DVB; C: 73.7 %, H: 6.4 %, Br: 18.0 %. 50% DVB; C: 80.8 %, H 6.7 %, Br: 10.0 %.

General procedure for click modification of modified P(S-DVB) microspheres. The modification of azide-functional particles prepared from P(S-DVB) containing 50 mass-% of DVB is given as an example. Azide-functional particles (100 mg, estimated amount of azides 4.3×10^{-5} mol), dry DMSO (5 mL), and CuBr (6.1 mg, 4.7×10^{-5} mol) were mixed in an argon atmosphere, followed by purging with argon for 5 min. Pentamethyldiethylenetriamine (PMDETA, 8.9 µL, 4.3×10^{-5} mol), triethylamine (5.9 µL, 4.3×10^{-5} mol) and alkyne-functional reagent (propargylamine, 10-undecynoic acid, or NBD-alkyne (**6**), 1.29×10^{-4} mol) were added. The reaction mixture was stirred for 48 h at room temperature before filtering and washing the particles with DMSO, water, ethanol, and acetone (25 mL each), followed by drying in vacuum. For P(DVB) microspheres (100 mg, estimated amount of azides 7.1×10^{-5} mol), a similar protocol was followed using PMDETA, CuBr, and triethylamine (7.1×10^{-5} mol each), and a three-fold excess of alkyne-functional reagent (2.1×10^{-4} mol). Click-modification of alkyne-functional microspheres followed the same protocol employing Rhodamine B azide (**7**) as reagent. Analytical data is presented and discussed in the main text.

7-Nitro-4-(prop-2-ynylamino)benzofuran (6).[49] To a solution of 4-chloro-7-nitro-benzofurazan (2.5 g, 12.5 mmol) in ethanol (20 mL) containing pyridine (1 mL, 12.5 mmol) was slowly added propargylamine (0.88 mL, 13.75 mmol) dissolved in ethanol (10 mL) while stirring and cooling with an ice bath for 30 min. The reaction was stirred for another 4 h at room temperature before evaporating the solvent and three co-evaporations with toluene to remove pyridine. The residue was diluted in THF and side products were removed by filtration. The filtrate was dried and purified by flash chromatography (petroleum spirit (b.p. 50–70 °C)–ethyl acetate 70:30) to afford an orange-brown solid (1.14 g, 5.2 mmol, 41.6 %) ^{1}H-NMR (400 MHz, DMSO-d_6) δ/ppm = 9.62 (1H, t, *J* = 5.6 Hz, N*H*), 8.61 (1H, d, *J* = 8.8 Hz, C*H*CNO_2), 6.47 (1H, d, *J* = 8.8 Hz, C*H*CNH), 4.33 (2H, s, CH_2), 3.35 (1H, t, *J* = 6.4 Hz, C*H*CCH_2); ^{13}C NMR (100 MHz, DMSO-d_6) δ/ppm = 144.4 (*C*NH), 143.9 (*C*=N), 137.5 (*C*HCNO_2), 122.2 (*C*NO_2), 100.3 (*C*HCNH), 78.5 (CH_2*C*CH), 75.1 (CH_2*C*CH), 32.4 (*C*H_2).

Rhodamin B Azide (7). 6-azido-1-hexanol (1.43 g, 10 mmol), prepared according to a literature procedure,[50] and Rhodamine B (3.2 g, 6.7 mmol) were dissolved in dry dichloromethane (50 mL). 4-(Dimethylamino)pyridine (DMAP, 0.80 g, 6.6 mmol) and *N*-(3-(dimethylamino)propyl)-*N'*-ethylcarbodiimide hydrochloride (EDC, 1.92 g, 10 mmol) were added and the reaction was stirred for 18 h at room temperature. The organic phase was then washed with 1 N HCl (3 ×), 1 N $NaHCO_3$ (3 ×) and brine (1 ×), dried over $MgSO_4$ and concentrated by evaporating ~90 % of the solvent. The red residue was diluted with THF (5 mL) and precipitated twice into diethyl ether (250 mL). The product was obtained by centrifugation as golden-purple solid (3.4 g, 85 %). FT-IR, ν/cm^{-1} = 2091 (C–N_3 stretching). ^{1}H-NMR (400 MHz, $CDCl_3$) δ/ppm = 8.25 (dd, 1H, *J* = 7.6 Hz, 1.2 Hz, COCC*H*), 7.74 (td, 2H, *J* = 7,6 Hz, 1.2 Hz, COCCCHC*H*), 7.71 (td, 2H, *J* = 7.6 Hz, 1.6 Hz, COCCHC*H*), 7.26 (dd, 1H, *J* = 7,6 Hz, 1.2

Hz, COCCC*H*), 7.05 (s, 1H, NCCHC*H*), 7.03 (s, 1H), 6.89 (dd, 2H, *J* = 5.6 Hz, 2.4Hz, NCC*H*CH), 6.77 (d, 2H, *J* = 1.6 Hz, NCC*H*C), 3.98 (t, 2H, *J* = 6.4 Hz, OCH_2), 3.61 (q, 8H, *J* = 6.8 Hz, $CH_2CH_2CH_2$), 3.19 (t, 2H, *J* = 6.8 Hz, N_3CH_2), 1.44 (m, 8H, CH_3CH_2N), 1.29 (t, 12H, *J* = 7.2 Hz, CH_3). ^{13}C NMR (100 MHz, $CDCl_3$) δ/ppm = 165.1 (*C*O), 158.9 (OCC*C*), 157.7 (O*C*), 155.6 (N*C*), 133.5 (COC*C*), 133.1 (COCCCH*C*H), 131.3 (COC*C*H), 130.4 (NCCH*C*H), 130.2 (COCCCH*C*H), 130.1 (COCC*C*H), 114.3 (NC*C*HCH), 113.5 (OC*C*), 96.3 (NC*C*HC), 65.5 (O*C*H_2), 51.3 (N_3CH_2), 46.2 (CH_3CH_2N), 28.6 (OCH_2CH_2), 28.2 ($N_3CH_2CH_2$), 26.3 ($CH_2CH_2CH_2$), 25.4 ($CH_2CH_2CH_2$), 12.7 (*C*H_3).

Characterization. Size distributions of PS seeds were measured with a disc centrifuge (DC24000, CPS Instruments Inc.) using an aqueous sucrose gradient. The instrument was calibrated with a polyvinylchloride (PVC) standard (0.476 μm) by CPS Instruments.

Surface morphology and uniformity of particles were monitored by scanning electron microscopy (SEM, LEO1525). A dispersion of particles in ethanol was generated through sonication and spread onto an aluminium specimen stub. Dried particles were coated with a thin layer of carbon in vacuum. Particle sizes and size distributions were calculated by measuring at least 100 particles using image J software.

Specific surface areas were determined by measuring nitrogen adsorption on a porosimeter (Thermo Scientific, Surfer) and calculated using Brunauer-Emmett-Teller theory.

Chemical transformations of microspheres were monitored by FT-IR spectroscopy on an ATR-FT-IR spectrometer Nicolet iS10 (Thermo Fisher Scientific) and by RAMAN spectroscopy performed on an RXN1 instrument (Kaiser Optical Systems, NCO Optics, 6.35 cm focus) at a wavelength of 785 nm and a power of 388 mW. RAMAN spectra were baseline corrected for easier interpretation.

Solution NMR spectra were measured on a Bruker Avance 400 spectrometer.

Solid state NMR experiments were performed on a Bruker Avance 400 spectrometer, equipped with a 4 mm double resonance probe. ^{13}C SPE and CP MAS spectra were acquired at an operating frequency of 100.66 MHz and a spinning frequency of 14 kHz. ^{13}C SPE MAS spectra were recorded using a 90° pulse of 4.1 µs and a 60 s repetition delay. A ^{13}C SPE MAS spectrum of an empty rotor was recorded under the same conditions and was used for background correction. ^{13}C CP MAS spectra were collected using a 90° pulse of 4.0 µs, a contact time of 2 ms, and a repetition delay of 5 s. The correction factor for CP MAS spectra was calculated by comparison of ^{13}C SPE and CP MAS spectra, following literature methods[51, 52] allowing for quantitative interpretation. The amount of residual double bonds in crosslinked P(S-DVB) particles was determined by comparison of the integral of the vinyl Ar–CH=*C*H_2 signal (112 ppm) with the integral of non-substituted aromatic carbons (144 ppm) considering that styrene contributes 5 and the DVB monomer mixture 4 non-substituted carbons, respectively.

CHN elemental analysis was performed on EuroVector Euro EA or Elementar Vario EL III instruments. Combustion gases were detected by a gas chromatography (Euro EA) or using a head conductivity detector (Vario EL III).

Bromine elemental analysis was performed through particle digestion by either of two methods; Schoeniger Oxidation or digestion with Na_2CO_3 and MgO,[45] each followed by potentiometric titration with $AgNO_3$, giving similar results. Results were further confirmed through bromine elemental analysis using an ion chromatography (IC) (ICS 1100 Dionex RFIC) instrument.

Confocal fluorescence microscopy images were captured on a home-made confocal laser scanning fluorescence microscopy setup using a Nd:YVO_4 laser with an excitation wavelength of

532 nm. Excitation light was focussed onto the sample with a 100×-lens (numerical aperture 0.8) and the fluorescence signal was detected by the same lens. Scattered light was blocked by a 532 nm long pass filter and the sample signal was detected by an avalanche photodiode.

Results and Discussion

Microsphere Synthesis

The synthesis of uniform crosslinked microspheres with varying porosity proceeded in several steps—precipitation polymerization synthesis of PS seeds, swelling of seeds with dibutylphthalate (DBP), styrene (S), and divinylbenzene (DVB), and polymerization of S–DVB inside the seeds. Precipitation polymerization of styrene was performed in ethanol with 2 wt% AIBN, 10 wt% polyvinylpyrrolidone (PVP-K30) and 4 wt% Aliquat 336 relative to the amount of styrene in the mixture as initiator and stabilizers, respectively. The ratio of monomer to solvent was varied between 10–20 vol%. Following polymerization overnight and purification by intense washing, the resulting particles were characterized by disc centrifuge and SEM. The former method, disc centrifuge (data shown in Figure 1) gave evidence of a very narrow size distribution with an average particle diameter of 2.2 ± 0.1 µm. SEM showed smooth spherical particles with an average diameter of 2.8 µm ± 0.1 µm, see Figure 2. This size and size distribution proved to be highly reproducible throughout several runs. The discrepancy of diameters between SEM and disc centrifuge measurements was attributed to the PVC-calibration of the disc centrifuge.

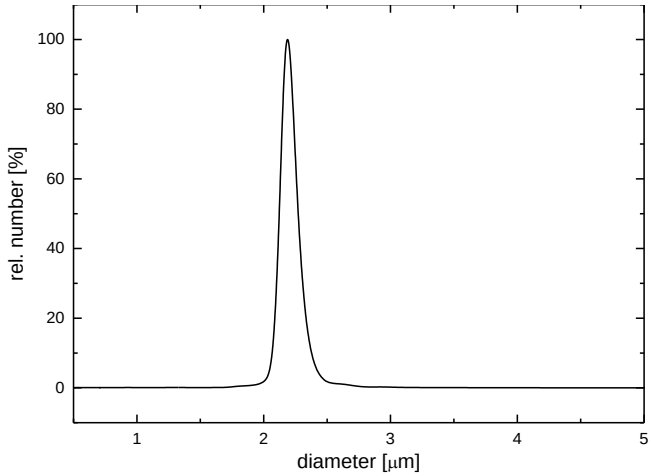

Figure 1. Disc centrifuge size distribution of seed particles indicating narrow size distribution

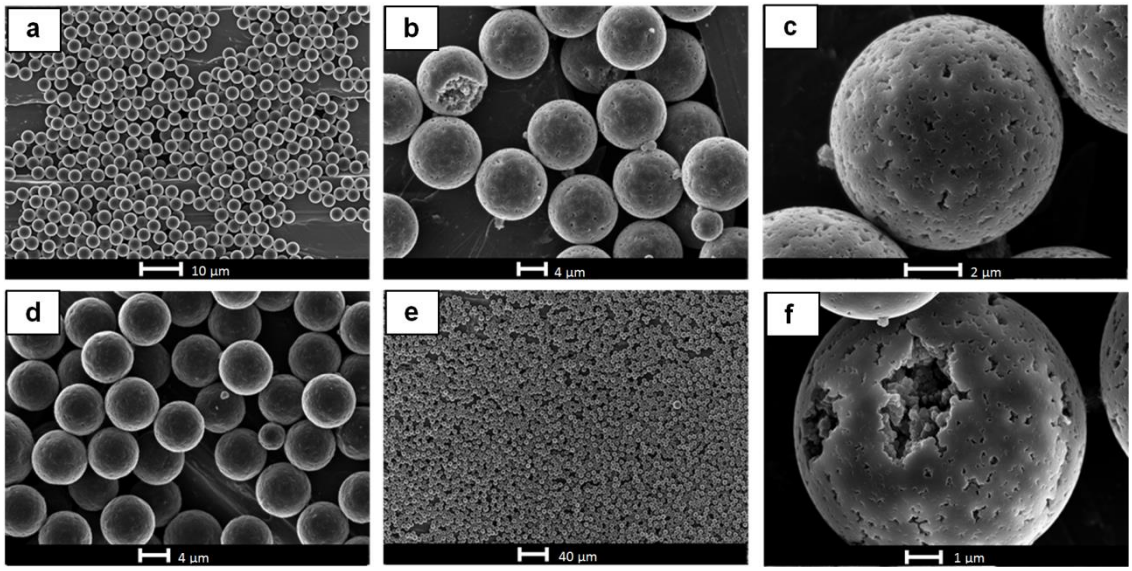

Figure 2. SEM images of polystyrene seed particles (a), microspheres MS3 with intermediate surface area (b,c), microspheres MS1 with low surface area (d), and high surface area microspheres MS6 (e,f). Smaller spherical particles in images (b) and (d) may suggest polymerisation of monomers outside of seed particles, while smaller pieces appear to result from breakage of particles through mechanical stress

Uniform porous P(S-DVB) microspheres (MS) were produced in a two-step swelling–polymerization procedure employing the polystyrene seed latexes. DBP was used in the first step as swelling agent with a ratio of 2.5 g DBP / 1 g PS seed particles followed by the addition of a mixture containing styrene monomer, DVB crosslinker, benzoylperoxide (BPO) initiator, as well as toluene which acted as porogen.[48] While the amount of porogen was kept constant the ratio of styrene–divinylbenzene was varied from 5:1 to 0:6, resulting in six microsphere batches, MS1–MS6, see Table 1 for monomer feed ratios. The swelling process and subsequent polymerization were monitored by optical microscopy (see supporting information) which allowed observation of DBP droplet disappearance (after ~4 h), concurrent swelling of seed particles to a constant diameter of 4.2 µm and growth and morphology change of particles during polymerization. After polymerization the resulting particles were purified by soxhlet extraction with water and THF to remove stabilisers and polystyrene seed material. Analysis by SEM indicated macroporous, spherical particles with narrow size distribution for all batches MS1–MS6, see Figure 2, suggesting that initiation and polymerization had occurred, as intended, inside the seed particles. The amount of DVB in the monomer feed had only limited influence on the microsphere size. With low DVB content, MS1 (S–DVB 5:1) and MS2 (S–DVB 4:2) had diameters of 6.6 ±0.2 µm and 7.6 ±0.2 µm, respectively. With higher DVB feed, however, MS3–MS6 all had similar diameters of ~8.6 ±0.2 µm, see Table 1, indicating a well-reproducible size range independent of monomer feed ratio. In contrast to diameters porosity varied significantly with the DVB feed content. Specific surface areas of microspheres determined by nitrogen adsorption spanned an impressive range from 11 m^2/g to 467 m^2/g increasing with DVB feed content in a nearly linear fashion, see Table 1 and Figure 3. This influence of DVB on

morphology was attributed to an earlier phase separation of P(S-DVB) polymer within the seeds due to a higher crosslinking density and resulting higher molecular weight.[53]

Table 1. Synthesis of Macroporous Microspheres (MS): Monomer–Crosslinker Feed Ratio, Diameter, and Specific Surface Area

Code	Styrene Feed [g]	DVB Feed [g]	D_n[a] [µm]	S[b] [m^2/g]
MS1	5	1	6.6 ±0.6	11
MS2	4	2	7.6 ±0.1	57
MS3	3	3	8.6 ±0.2	65
MS4	2	4	8.5 ±0.5	267
MS5	1	5	8.7 ±0.2	398
MS6	0	6	8.6 ±0.2	467

[a] number average diameter determined by SEM; standard deviation from measuring at least 100 particles, [b] specific surface area determined by BET nitrogen adsorption

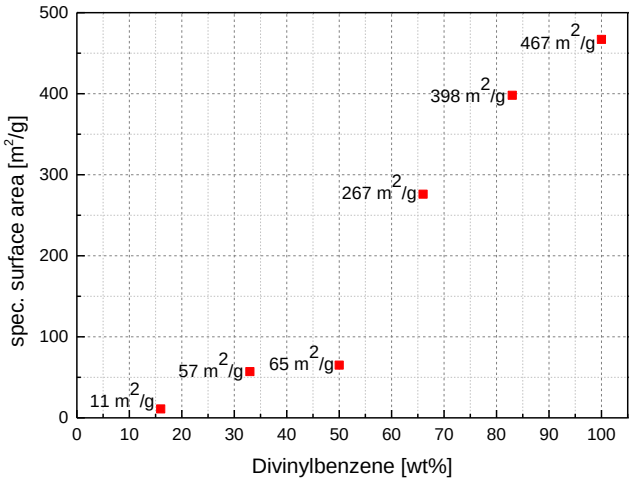

Figure 3. Specific surface areas of microspheres determined by BET nitrogen adsorption in dependence of DVB crosslinker feed.

Microsphere functionalization

With a library of uniform P(S-DVB) microspheres with tuneable surface area in hand, we next investigated their modification. For most applications requiring functional microspheres not

only high specific surface area but also surface accessibility is important. In order to study efficiency of particle surface modification we chose CuAAC click chemistry as a robust method with a well-documented comprehensive scope and because the respective reactants, azide and alkyne functionality, are accessible through modification of residual double bonds. Firstly, we quantified the amount of residual double bonds of three samples, MS1, MS3 and MS6 by ^{13}C solid state CP-MAS NMR spectroscopy (SSNMR) which allowed for sufficient resolution and integration of signals.[51] Molar amounts were determined by comparison of the integrals of remaining vinyl groups at 112 ppm (–CH=*C*H_2) with the integrals of non-substituted aromatic carbons, the number of the latter being dictated by the S–DVB ratio. For MS1, the sample with lowest (16.7 wt%) DVB feed content, no quantifiable signal was observed in SSNMR suggesting (nearly) complete polymerization of all DVB vinyl groups. For MS3 and MS6 (both with diameters of 8.6 µm but differing specific surface areas), residual double bonds were clearly visible through SSNMR and could be quantified. For sample MS3 (S–DVB55 50:50 by mass, average of 24.5 mol-% of DVB crosslinkers per monomer in feed) an average of 0.17 remaining vinyl groups per monomer unit was found in the particles, indicating in a degree of crosslinking of 7.5% and corresponding to a remaining double bond concentration of 1.47 mmol/g, see Table 2. For sample MS6 (100% DVB55) a crosslinking density of 31% and a loading of 2.37 mmol/g of residual double bonds was determined by SSNMR confirming both the aforementioned higher degree of crosslinking (which affects the observed morphology) and a higher amount of residual double bonds. Residual double bonds of microspheres MS3 and MS6 were next subjected to modification into azides and alkynes, respectively, see Scheme 1.

Table 2. Overview of Parameters of Samples MS3 and MS6, Modification to Azide and Alkyne Functionality and Click Modification

	MS3	**MS6**
monomer feed ratio [mass-%]	S–DVB 50:50	S–DVB 0:100
residual double bonds per average monomer unit	0.17[a]	0.31[a]
residual double bond loading	1.47 mmol/g[a]	2.37 mmol/g[a]
degree of crosslinking	7.5%[a]	24%[a]
conversion of double bond hydrobromination	quant.[a]	quant.[a]
conversion of bromide substitution by azide	32%[b]	35%[a,b]
azide loading	0.43 mmol/g	0.71 mmol/g
azide concentration in particles	5.5 mol%	10.9 mol%
CuAAC conversion with propargylamine	100%[c]	90%[c]
CuAAC conversion with 10-undecynoic acid	91%[c]	71%[c]
CuAAC conversion with NBD-alkyne (**6**)	85%[c]	67%[c]
conversion of double bond bromination	quant.[d]	98%[d]
conversion of dibromide double dehydrohalogenation	53%[d]	41%[d]
alkyne loading	0.70 mmol/g[d,e]	0.78 mmol/g[d,e]
alkyne concentration in particles	9.0 mol%	12.4 mol%
CuAAC conversion with Rhodamine-azide (**7**)	quant.[e]	quant.[e]

[a] determined by solid state NMR taking into account the concentration of divinylbenzene in the commercial 55% grade monomer; [b] calculated from nitrogen elemental analysis; [c] estimated from remaining azide signal in FT-IR spectra; [d] calculated from bromine IC elemental analysis; [e] presence and conversion of alkynes was confirmed by RAMAN spectroscopy

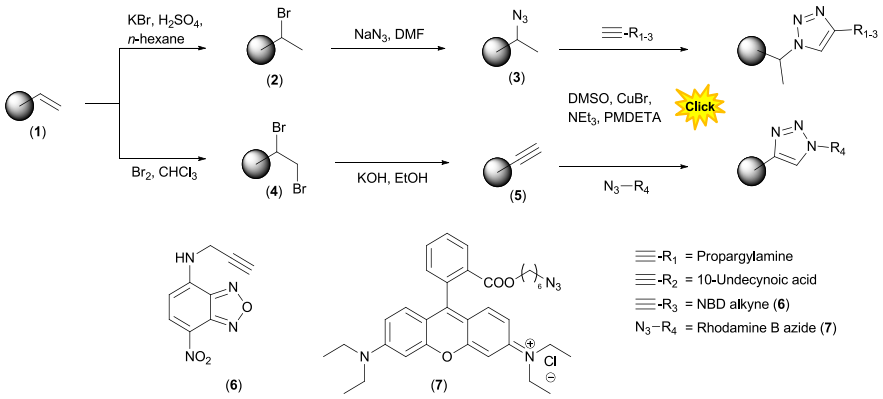

Scheme 1. Synthetic overview of microsphere functionalization with azide (top) and alkyne (bottom) functionality and click-modification; structures of fluorescent alkyne and azide-functional dyes

Introduction of Azide Functionality and Click-Modification

Surface-bound azide functionality was produced in a two-step procedure involving hydrobromination of vinyl groups into 1-bromoethyl groups followed by bromide substitution by azide, a procedure documented for the modification of P(S-DVB) particles.[35, 45] We monitored the success of these reactions by means of SSNMR, FT-IR spectroscopy, elemental combustion analysis (CHN), and bromine IC elemental analysis. Results are summarised in Table 2.

The first step, addition of HBr gas to double bonds, proceeded quantitatively for both samples MS3 and MS6. SSNMR spectra of the native porous microspheres MS6 containing residual double bonds and of particles after HBr treatment are shown in Figure 4. The spectra show the complete disappearance of signals arising from the vinyl groups suggesting full conversion. The spectrum of the hydrobrominated microspheres additionally shows a signal at 26 ppm characteristic of a methyl group adjacent to a brominated carbon (–CHBr–CH_3) confirming the expected formation of 1-bromoethyl Markovnikov adducts. Analogous spectra of microspheres

MS3 are shown in the supporting information. Successful hydrobromination was also confirmed by FT-IR spectroscopy, Figure 5, through the disappearance of a signal at 901 cm^{-1} attributed to C=C bending vibration characteristic of vinyl groups.

In the second step bromide functionality was substituted by azide groups under standard conditions employing sodium azide in DMF–water. After reaction an FT-IR spectrum (Figure 5, curve c) qualitatively confirmed the incorporation of azide functionality into porous microspheres through the appearance of a strong absorbance band at 2101 cm^{-1} which was attributed to the characteristic azide N=N stretching vibration. An SSNMR spectrum of the azide-functional microspheres showed an additional peak at 61 ppm (Figure 4), characteristic of the $–CHN_3–CH_3$ segment. Integration of this signal indicated a content of ~11 mol% of azidomethylstyrene units. Elemental analysis of the azide-functional microspheres revealed a nitrogen content of 3.0 mass-%. From these values an efficiency of the azide substitution reaction of 35% was estimated. The resulting microspheres would thus have a molar composition of 45 mol-% of ethylstyrene units (impurity in DVB55), 24 mol-% of crosslinked DVB units (degree of crosslinking determined by SSNMR on original microspheres), 20.1 mol-% of residual 1-bromoethylstyrene units, and 10.9 mol-% of 1-azidoethylstyrene units (corroborating the SSNMR result) and, with a loading of 0.71 mmol/g azides, confirming the observed mass percentage of 3 mass% nitrogen. Additionally, a calculated mass percentage of 10.6 mass% Br for this molar composition matched well with a content of 11.0% as observed by bromine IC elemental analysis underpinning the estimated reaction efficiency. A similar bromide substitution efficiency of 32% was estimated for microspheres MS3 resulting in an azide loading of 0.43 mmol/g. Because of the relatively high molar mass of the residual bromide containing units azide loading was also expressed in a molar percentage (5.5 mol% for MS3, see

table 2) which serves better to illustrate and compare reaction efficiencies than the more commonly used amount-per-mass loading value. We attribute the incomplete bromide substitution to a certain amount of bromide groups being inaccessible for the azide reagent which is potentially related to disparate polarities of ionic sodium azide (which, in water–DMF can be expected to be hydrated by a water sphere) and the nonpolar P(S-DVB) microspheres. While this bromo–azide substitution reaction is typically assumed to proceed quantitatively on microparticles we note that supporting analytical data is not always presented. Nevertheless, even at conversions of 32–35%, microspheres with reasonably high loading of functional azide groups were prepared.

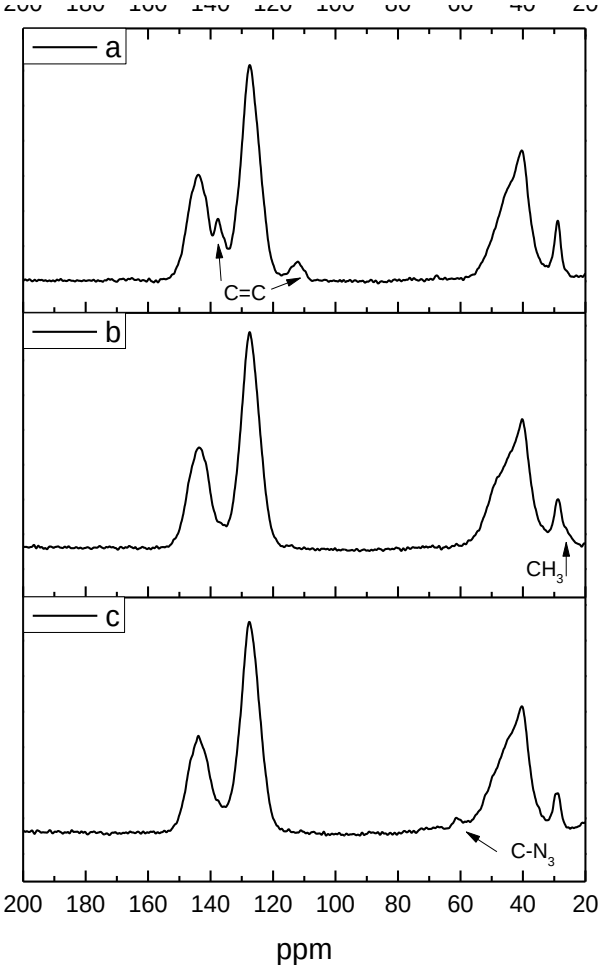

Figure 4. Solid state NMR spectra of porous particles MS6 exhibiting residual vinyl groups (a), after hydrobromination showing disappearance of vinyl groups and a shoulder at 26 ppm (–CHBr–CH_3) (b), and after bromide substitution by azide displaying a characteristic signal at 61 ppm (–CHN_3–CH_3) (c).

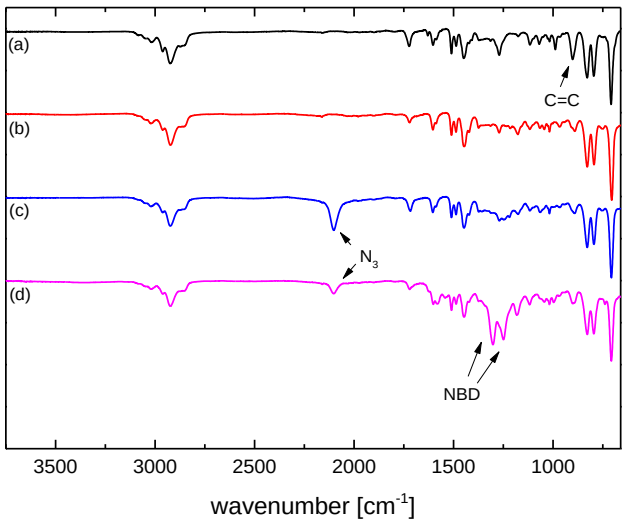

Figure 5. FT-IR spectra of porous particles MS6 (a), after hydrobromination (b), after bromide substitution with azide (c), and after clicking with NBD-alkyne (**6**) (d), with characteristic bands assigned.

We next investigated the modification of azide-functional microspheres in CuAAC reactions. Three alkyne substrates carrying different functionality were chosen as models to illustrate the scope of click-modification. Propargylamine and 10-undecynoic acid were chosen as commercially available functional alkynes, while an alkyne-functional fluorescent dye, 7-nitro-4-(prop-2-ynylamino)benzofuran, NBD alkyne (compound **6** in Scheme 1) was synthesised to allow for optical analysis. Reactions were performed under standard conditions using the alkyne reagents in slight excess and CuBr, pentamethyldiethylenetriamine (PMDETA), triethylamine, and DMSO as catalyst, ligand, auxiliary base, and solvent, respectively. Because of the strong infrared absorbance of the azide functionality, FT-IR spectroscopy served as an expedient means to monitor the success of microsphere click reactions. Assuming that azide functionality was only consumed through the intended formation of triazole linkages the relative reduction of the azide band in normalised FT-IR spectra was used to estimate CuAAC conversions—values for

the three substrates are given in table 2. For the modification of microspheres MS3 with propargylamine, the smallest reagent, complete disappearance of the azide absorption band in IR was observed, indicating accessibility and conversion of all azide groups. Two trends emerge from the modification of MS3 and MS6 with the other substrates. (i) Conversion decreases with an increasing size of the alkyne substrates, possibly due to steric hindrance within the microsphere pores. (ii) Conversions on microspheres MS6 with a higher crosslinking degree are slightly lower ranging from 90% for propargylamine to 67% for NBD alkyne, possibly due to lower pore accessibility compared to the MS3 sample. Nevertheless, even at a conversion of 67% the resulting NBD dye-functional particles contained ~7.3 mol-% of dye-modified monomer units corresponding to a loading of 0.43 mmol/g dye functionality. This modification was sufficient to observe characteristic infrared absorbance bands of the NBD group in the modified particles at 1301 and 1249 cm^{-1}, see Figure 5, curve d. NBD-modified particles also clearly showed the yellow-brown colour of the attached dye as shown in an optical photograph in Figure 6.

Figure 6. Optical photograph (A) of unmodified porous microspheres (left), microspheres after azide modification and click-attachment of NBD alkyne (middle), and alkyne-modified microspheres after click-attachment of Rhodamine B azide (right); dark field microscopy image (B) of Rhodamine B labelled microspheres MS6 (scale bar = 50 μm).

Introduction of Alkyne Functionality and Click-Modification

As mentioned above introduction of azides into microspheres is by far the most common synthetic approach toward click-modification. Here, we also investigated the introduction of alkyne functionality into microspheres which was achieved, in two steps, by means of residual double bond bromination followed by double dehydrohalogenation, see Scheme 1. In addition to SSNMR and bromine IC elemental analysis, Raman spectroscopy served as an expedient tool to follow the modification of particles.

The first step, addition of bromine to double bonds, proceeded with very high to quantitative yield for both samples of microspheres, MS3 and M6, as evidenced by bromine IC elemental analysis. For example, after treating microspheres MS6 with bromine, a content of 27 mass-% of bromine was measured. Taking the amount of residual double bonds in unmodified microspheres MS6 (as determined by SSNMR) into consideration, the observed bromine mass percentage in modified particles corresponded to a conversion of 98% of double bonds into 1,2-dibromoethyl species. For microspheres MS3 a quantitative conversion was estimated from elemental analysis. For both samples disappearance of double bonds was also observed by SSNMR, see supporting information. Addition of bromine to double bonds is a well-documented method in quantitative analysis and the calculated (near) quantitative conversions support the accuracy of double bond determination in the original particles by SSNMR.

In a second step, 1,2-dibromoethyl moieties were transformed into alkyne groups by means of double elimination of HBr using KOH in ethanol. Raman spectroscopy confirmed the formation of alkyne groups through a characteristic alkyne absorbance at 2109 cm^{-1}, see exemplary spectra of MS3 microspheres in Figure 7. Quantitative data was obtained from bromine IC elemental analysis; measured values of 18 mass% Br for MS6 and 10 mass% for MS3 corresponded to

double elimination efficiencies of 41% (MS6) and 53% (MS3), respectively. Of note, two-step modification of remaining double bonds into alkynes proceeded with higher overall conversion than the two-step modification into azide functionality. Porous microspheres with 0.70 mmol/g and 0.78 mmol/g alkyne functionality were thus obtained from microspheres MS3 and MS6, respectively. The similar mass loadings for both samples stem from the high molar mass of the remaining dibromide units which effectively reduce the functionality-per-mass ratio for the MS6 sample; molar alkyne loadings are given in Table 2.

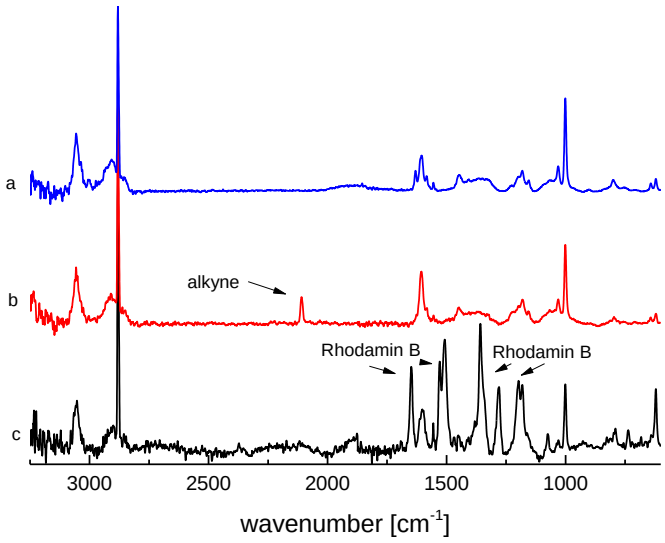

Figure 7. Raman spectra of porous vinyl-functional particles MS3 (a), after two-step modification to propargyl-functional microspheres showing alkyne functionality (b), and after click-modification with Rhodamine B azide (**7**) (c) with assignment of characteristic bands

We next investigated the modification of the particle-bound alkyne groups by CuAAC clicking. As reagent we equipped the fluorescent dye Rhodamine B with an azide function tethered by a C6 spacer (structure **7** in Scheme 1). CuAAC was performed under the same

conditions as detailed above for the 'inverse' coupling on particle-bound azide groups. Particles were purified by repeated washing until washing solvents remained colourless and IR spectroscopy gave no evidence of remaining azide groups suggesting full removal of non-covalently attached Rhodamine B reagent. Apart from optical confirmation—the resulting microspheres were brightly pink, see Figure 6—Raman spectroscopy showed strong new signals between 1648 and 1181 cm^{-1} associated with Rhodamine B as well as the complete disappearance of the alkyne signal, suggesting full conversion. Given the higher alkyne loading compared to the azide-functional particles and the size of the Rhodamine B azide reagent, complete conversion of all alkyne groups was somewhat surprising. Notably, Raman spectroscopy only provides information on sample surface areas that are accessible by a laser beam and suited for the detection of Raman scattering events, which can be expected to be limited to the outer layer of microspheres, where, at least, alkyne groups appear to have been quantitatively converted. As mentioned above, accessibility and utilisation of the high surface area *inside* particles is, however, of great interest. Using the click modification with Rhodamine B azide as a model to determine accessibility of the inside of microspheres, we subjected the resulting dye-labelled microspheres to confocal scanning microscopy. Observing the fluorescence signal of the dye labels, this method allowed mapping relative functionalization efficiency within cross-sectional slices of microspheres, see Figure 8. In order to analyse the core of microspheres, slices were measured approximately through the equator of particles, with observed slice diameters matching particles diameters determined by SEM (see table 1). The cross-sectional profile of dye-labelled microspheres MS3, representative image in Figure 8ab, indicates dye labelling throughout the particle, including the core, suggesting that all three chemical transformations—bromination, double elimination, and CuAAC coupling—had

occurred, at least to some extent, throughout the thickness of particles. The edge of the particles, to a depth of ~ 1 μm displayed approximately 2-fold higher fluorescence intensity than the rather homogeneously fluorescing inside of the particles. This observation supports full alkyne conversion leading to high dye density on the outer layer of particles as suggested by Raman spectroscopy and indicates that incomplete transformations (such as double elimination) appeared to suffer from poor conversion within the core of the particles. We assume particles to possess a core with higher crosslinking density which can be expected to limit mass transport leading to lower surface accessibility within the particles. A similar, though less pronounced, cross-sectional fluorescence profile was observed for dye-labelled microspheres MS6, which likewise showed higher fluorescence intensity in the outer 1–2 μm thick layer, again suggesting higher accessibility of this region for chemical modification. Overall, microspheres MS6 showed higher fluorescence intensity, especially within the cores of particles, compared to microspheres MS3. This reflects the overall higher surface area and higher functionalization density of these particles made from 100% DVB. Localised areas of higher fluorescence intensity within both microspheres MS3 and MS6 are assumed to reveal the structure of macropores within particles.

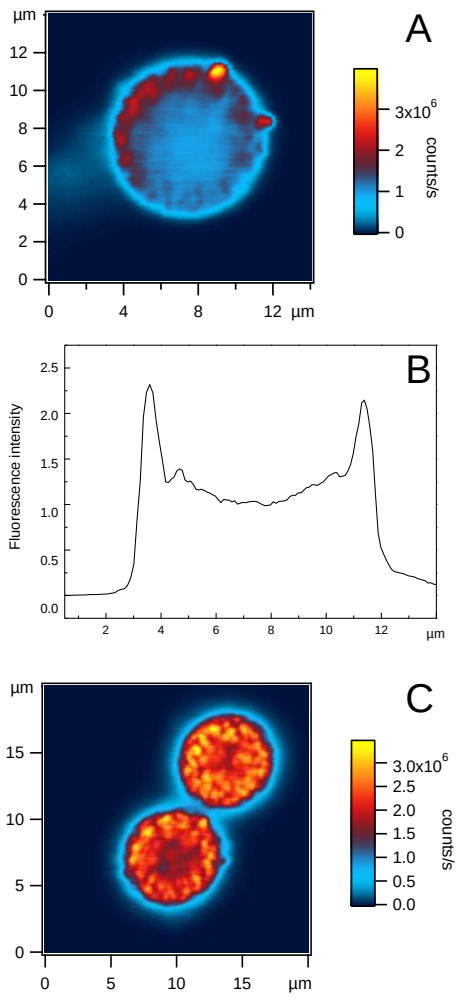

Figure 8. Confocal laser scanning microscopy image of Rhodamine B labelled microspheres MS3 (A) and fluorescence intensity cross-section (B) of the particle indicating higher dye concentration in the outer layer and within macropores; confocal laser scanning microscopy image (C) of Rhodamine B labelled microspheres MS6 indicating dye labelling throughout the particle with higher concentration within macropores.

Conclusions

While 'clickable' macroporous particles present ample opportunity for application, only limited studies have presented quantitative data on the efficiency of chemical transformation of residual double bonds. With diameters of several micrometres and highly crosslinked cores, P(S-DVB) microspheres present challenges for complete postpolymerization modification. Indeed, while hydrobromination and bromination each proceeded to (near) completetion, the respective seconds steps toward azide and alkyne functionality (bromo–azide substitution and double elimination, respectively), suffered from lower conversion. Nevertheless, functional microspheres containing up to 10.9 mol% of azide-functional monomer units or up to 12.4 mol-% of alkyne functional monomer units were obtained, signifying the overall slightly higher efficiency of the alkyne functionalization route. The functional particles allowed for modification via CuAAC click chemistry with a variety of model reagents. Confocal laser scanning microscopy indicated a higher dye labelling within the outer layer of particles suggesting a core–shell structure with the core being chemically less accessible for the double elimination and/or the CuAAC modification reaction. For particles with higher surface area (higher DVB content), less difference between core- and shell functionalization was found, with a high degree of functionalization throughout the entire thickness of the particles, suggesting particles with higher DVB content to be preferable for applications requiring large surfaces areas. Results show that macroporous P(S-DVB) particles offer a very large—and accessible—surface area with the potential of tailored functionalization, as demonstrated here by click chemistry.

Acknowledgements.

The authors thank Aina Reich for confocal laser scanning fluorescence microscopy measurements (Physical Chemistry, University of Hamburg) and Renate Walter (Zoological Institute, University of Hamburg) for SEM image measurements. P.J.R. acknowledges the Australian Research Council (ARC) for funding through a Discovery Early Career Researcher Award (DE120101547). M.A., W. P., and H.-U.M. acknowledge the German Federal Ministry of Education and Research (BMBF) for financial support (13N11312).

References

1. Y. Li, F. Gao, W. Wei, J.-B. Qu, G.-H. Ma and W.-Q. Zhou, *J. Mol. Catal.-Enzym.*, 2010, **66**, 182-189.
2. Q. Liu, Y. Li, S. Shen, Q. Xiao, L. Chen, B. Liao, B. Ou and Y. Ding, *J. Appl. Polym. Sci.*, 2011, **121**, 654-659.
3. O. Okay, *Prog. Polym. Sci.*, 2000, **25**, 711-779.
4. M. R. Buchmeiser, *J. Chromatogr. A*, 2001, **918**, 233-266.
5. F. M. B. Coutinho, M. A. F. S. Neves and M. L. Dias, *J. Appl. Polym. Sci.*, 1997, **65**, 1257-1262.
6. S. Punna, E. Kaltgrad and M. G. Finn, *Bioconjugate Chem.*, 2005, **16**, 1536-1541.
7. M. Slater, M. Snauko, F. Svec and J. M. J. Fréchet, *Anal. Chem.*, 2006, **78**, 4969-4975.
8. E. Unsal, S. T. Camli, S. Senel and A. Tuncel, *J. Appl. Polym. Sci.*, 2004, **92**, 607-618.
9. M. Benaglia, A. Puglisi and F. Cozzi, *Chem. Rev.*, 2003, **103**, 3401-3430.
10. A. Kirschning, H. Monenschein and R. Wittenberg, *Angew. Chem.*, 2001, **113**, 670-701.
11. N. Miletić, Z. Vuković, A. Nastasović and K. Loos, *J. Mol. Catal.-Enzym.*, 2009, **56**, 196-201.
12. M. T. Gokmen and F. E. Du Prez, *Prog. Polym. Sci.*, 2012, **37**, 365-405.
13. B. Thomson, A. Rudin and G. Lajoie, *J. Appl. Polym. Sci.*, 1996, **59**, 2009-2028.
14. J. Ugelstad, A. Berge, T. Ellingsen, O. Aune, L. Kilaas, T. N. Nilsen, R. Schmid, P. Stenstad, S. Funderud, G. Kvalheim, K. Nustad, T. Lea, F. Vartdal and H. Danielsen, *Makromol. Chem.-M. Symp.*, 1988, **17**, 177-211.
15. J. Ugelstad, K. H. Kaggerud, F. K. Hansen and A. Berge, *Makromol. Chem.*, 1979, **180**, 737-744.
16. J. Ugelstad, H. R. Mfutakamba, P. C. Mørk, T. Ellingsen, A. Berge, R. Schmid, L. Holm, A. Jørgedal, F. K. Hansen and K. Nustad, *J. Polym. Sci. Pol. Symp.*, 1985, **72**, 225-240.
17. J. Ugelstad, P. C. Mórk, K. H. Kaggerud, T. Ellingsen and A. Berge, *Adv. Colloid Interfac.*, 1980, **13**, 101-140.
18. M. Okubo, E. Ise and T. Yamashita, *J. Polym. Sci. Pol. Chem.*, 1998, **36**, 2513-2519.
19. M. Okubo and T. Nakagawa, *Colloid Polym. Sci.*, 1992, **270**, 853-858.
20. M. Okubo, M. Shiozaki, M. Tsujihiro and Y. Tsukuda, *Colloid Polym. Sci.*, 1991, **269**, 222-226.

21. C. M. Cheng, F. J. Micale, J. W. Vanderhoff and M. S. El-Aasser, *J. Polym. Sci. Pol. Chem.*, 1992, **30**, 235-244.

22. C. M. Cheng, J. W. Vanderhoff and M. S. El-Aasser, *J. Polym. Sci. Pol. Chem.*, 1992, **30**, 245-256.

23. Q. C. Wang, F. Švec and J. M. J. Fréchet, *J. Polym. Sci. Pol. Chem.*, 1994, **32**, 2577-2588.

24. R. A. Prasath, M. T. Gokmen, P. Espeel and F. E. Du Prez, *Polym. Chem.*, 2010, **1**, 685-692.

25. S. Xu, Z. Nie, M. Seo, P. Lewis, E. Kumacheva, H. A. Stone, P. Garstecki, D. B. Weibel, I. Gitlin and G. M. Whitesides, *Angew. Chem. Int. Ed.*, 2005, **44**, 724-728.

26. D. R. Breed, R. Thibault, F. Xie, Q. Wang, C. J. Hawker and D. J. Pine, *Langmuir*, 2009, **25**, 4370-4376.

27. M. Kedem and S. Margel, *J. Polym. Sci. Pol. Chem.*, 2002, **40**, 1342-1352.

28. A. Unciti-Broceta, E. M. Johansson, R. M. Yusop, R. M. Sanchez-Martin and M. Bradley, *Nat. protoc.*, 2012, **7**, 1207-1218.

29. J. M. J. Fréchet and M. J. Farrall, in *Chemistry & Properties of Crosslinked Polymers*, ed. S. S. Labana, Academic Press, 1977, pp. 59-83.

30. M. Bacquet, C. Caze, J. Laureyns and C. Bremard, *Reactive Polymers, Ion Exchangers, Sorbents*, 1988, **9**, 147-153.

31. R. S. Feinberg and R. B. Merrifield, *Tetrahedron*, 1974, **30**, 3209-3212.

32. A. R. Mitchell, S. B. H. Kent, M. Engelhard and R. B. Merrifield, *J. Org. Chem.*, 1978, **43**, 2845-2852.

33. J.-P. Montheard, M. Chatzopoulos and M. Camps, *J. Macromol. Sci.-Pol R*, 1988, **28**, 503-592.

34. B. R. Stranix, J. P. Gao, R. Barghi, J. Salha and G. D. Darling, *J. Org. Chem.*, 1997, **62**, 8987-8993.

35. K. L. Hubbard, J. A. Finch and G. D. Darling, *React. Funct. Polym.*, 1999, **39**, 207-225.

36. K. L. Hubbard, J. A. Finch and G. D. Darling, *React. Funct. Polym.*, 1999, **42**, 279-289.

37. A. S. Goldmann, A. Walther, L. Nebhani, R. Joso, D. Ernst, K. Loos, C. Barner-Kowollik, L. Barner and A. H. E. Müller, *Macromolecules*, 2009, **42**, 3707-3714.

38. V. V. Rostovtsev, L. G. Green, V. V. Fokin and K. B. Sharpless, *Angew. Chem. Int. Ed.*, 2002, **41**, 2596-2599.

39. W. H. Binder and R. Sachsenhofer, *Macromol. Rapid Commun.*, 2007, **28**, 15-54.

40. W. H. Binder and R. Sachsenhofer, *Macromol. Rapid Commun.*, 2008, **29**, 952-981.

41. K. Kempe, A. Krieg, C. R. Becer and U. S. Schubert, *Chem. Soc. Rev.*, 2012, **41**, 176-191.

42. J. E. Moses and A. D. Moorhouse, *Chem. Soc. Rev.*, 2007, **36**, 1249-1262.

43. B. S. Sumerlin and A. P. Vogt, *Macromolecules*, 2010, **43**, 1-13.

44. C. E. Evans and P. A. Lovell, *Chem. Commun.*, 2009, 2305-2307.

45. B. Karagoz, Y. Y. Durmaz, B. N. Gacal, N. Bicak and Y. Yagci, *Des. Monomers Polym.*, 2009, **12**, 511-522.

46. A. K. Oyelere, P. C. Chen, L. P. Yao and N. Boguslavsky, *J. Org. Chem.*, 2006, **71**, 9791-9796.

47. M. T. Gokmen, W. Van Camp, P. J. Colver, S. A. F. Bon and F. E. Du Prez, *Macromolecules*, 2009, **42**, 9289-9294.

48. S. T. Camli, E. Unsal, S. Senel and A. Tuncel, *J. Appl. Polym. Sci.*, 2004, **92**, 3685-3696.

49. J. M. Katzenstein, D. W. Janes, J. D. Cushen, N. B. Hira, D. L. McGuffin, N. A. Prisco and C. J. Ellison, *ACS Macro Letters*, 2012, **1**, 1150-1154.

50. X. Wei, W. Chen, X. Chen and T. P. Russell, *Macromolecules*, 2010, **43**, 6234-6236.

51. M. Gaborieau, L. Nebhani, R. Graf, L. Barner and C. Barner-Kowollik, *Macromolecules*, 2010, **43**, 3868-3875.

52. R. V. Law, D. C. Sherrington and C. E. Snape, *Macromolecules*, 1997, **30**, 2868-2875.

53. M. Galia, F. Svec and J. M. J. Frechet, *J. Polym. Sci. Pol. Chem.*, 1994, **32**, 2169-2175.